ACS APPLIED MATERIALS & INTERFACES

RESEARCH ARTICLE

www.acsami.org

Change in Electronic States in the Accumulation Layer at Interfaces in a Poly(3-hexylthiophene) Field-Effect Transistor and the Impact of Encapsulation

Byoungnam Park,*[,†] Y. J. Kim,[‡] Samuel Graham,[‡,§] and Elsa Reichmanis*[,†,§,⊥]

[†]School of Chemical and Biomolecular Engineering, [‡]George W. Woodruff School of Mechanical Engineering, [§]School of Materials Science and Engineering, and [⊥]School of Chemistry and Biochemistry, Georgia Institute of Technology, Atlanta, Georgia 30332, United States

ABSTRACT: The electrical properties of organic field-effect transistors (OFETs) are largely determined by the accumulation layer that extends only a few molecular layers away from the gate dielectric/organic semiconductor interface. To understand degradation processes that occur within the device structure under ambient conditions, it is thus essential to probe the interface using an architecture that minimizes the effects of bulk transport of contaminating species through upper layers of material in a thick film device. Using FETs designed with multiple voltage probes along the conducting channel and an ultrathin film of the active material, we found that the charge carrier density and the FET mobility decrease, and further, the contact and channel properties are strongly correlated. FET devices prepared with an ultrathin film of P3HT become significantly contact limited in air due to a hole diffusion barrier near the drain electrode. Encapsulation of the device with a layered organic/inorganic barrier material consisting of parylene and Al_2O_3 appreciably retarded diffusion of molecular species from ambient air into P3HT.

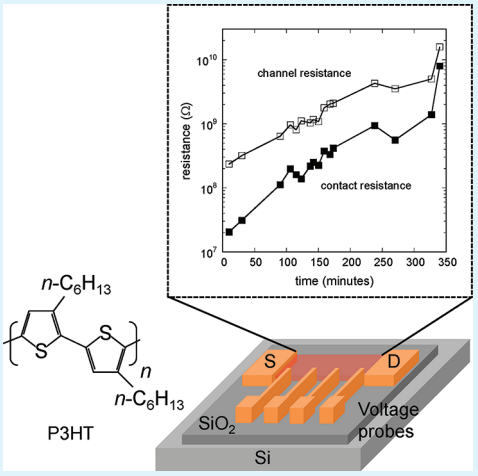

KEYWORDS: organic field-effect transistor, conjugated polymer, degradation, interface, encapsulation, P3HT

INTRODUCTION

Organic semiconductors are the essential charge carrying component in organic electronic devices such as organic field-effect transistors (OFETs), organic light-emitting diodes (OLEDs), and organic solar cells (OSCs).[1−3] Solution-processable conjugated polymers in particular have attracted significant interest because they offer the promise of cost-effective fabrication of all of the building blocks required for device operation.[4,5] However, the low ionization potentials of conjugated polymers, with poly(3-hexylthiophene) (P3HT) being a representative example, make such materials vulnerable to oxidative doping under ambient conditions; a process that degrades their carrier transport properties.[6,7] The poor air stability of the materials thus reduces overall flexibility in design and optimization of devices that incorporate conjugated polymers by limiting the choice of active material.

The air stability of conjugated polymers employed in organic devices has been the subject of intense interest.[7,8] Water and oxygen have been identified as the dominant causes of device degradation. For instance, it has been shown that these molecules can diffuse through pinholes present in inorganic electrodes and subsequently react with the organic active elements. Particularly for OSCs and OLEDs, chemical and photochemical degradation cause an initial rapid decay in performance and were shown to emanate from the interaction of both water and oxygen species with semiconducting polymers and metal electrodes.[8]

A bottom-contact FET that is very sensitive to electronic structural changes at the metal/organic semiconductor and organic semiconductor/gate dielectric interfaces can provide an effective test vehicle to explore the effect of ambient conditions on the electrical properties of a single organic semiconductor layer. Such information will be critical for understanding environmental effects on semiconductor performance, which in turn will inform the design and development of robust materials for OFET, OSC, and OLED applications. Through use of an FET device architecture, changes in the mobility and current with respect to time have been investigated in controlled environments.[9,10] It is known that water decreases the drain current in P3HT based FETs by capturing charge carriers, whereas oxygen increases the current by producing holes in the semiconductor.[11,12] These opposing effects of water and oxygen have been reported for FETs fabricated with relatively thick layers of the conjugated polymer where the thickness was in the range of tens of nanometers.[13,14]

To develop a clear understanding of the connection between the observed changes in transistor parameters, including device mobility and threshold voltage, and changes in the electronic

Received: June 13, 2011
Accepted: August 24, 2011
Published: August 24, 2011

dx.doi.org/10.1021/am200760m | *ACS Appl. Mater. Interfaces* 2011, 3, 3545–3551

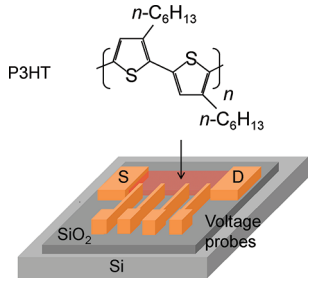

Figure 1. Schematic diagrams of the molecular structure of P3HT and the FET device configuration incorporating multiple voltage probes used in this study. The arrow points to the semiconductor thin film.

states within the semiconducting layers induced by relevant components in ambient air, it is highly desirable to use an ultrathin organic film for the conducting channel. It is precisely the electronic and structural properties of the semiconducting film directly adjacent to the gate dielectric that governs device properties/performance. In FETs fabricated with relatively thick films of an organic semiconductor, the semiconductor/gate dielectric interface is buried such that the direct observation of the variation of field effect conductance due to degradation of the interface is suppressed by the change in the bulk conductance that results from the interaction between upper layers of the film and airborne species. Further, morphological differences in the channel and contact regions that allow for degradation mechanisms that are not identical, require separate studies of the contact and channel properties. Such studies have not been performed on solution-processed conjugated polymers.

To understand degradation mechanisms associated with solution processed conjugated polymers in ambient air, we structured a bottom-contact FET using P3HT as a model semiconductor. The P3HT film thickness was comparable to the thickness of the charge accumulation layer. The electronic structural changes in the P3HT layer, close to the gate dielectric and near the metal contacts, are interrogated through analysis of the variations in the contact and channel properties observed for a device configured with multiple voltage probes between the source and drain electrodes. To suppress the degradation process that occurs in ambient air, we encapsulated the interfaces, thereby effectively stabilizing the Au/P3HT contact and P3HT conducting channel transport properties.

The device configuration in which voltage probes are fabricated between electrodes, as shown in Figure 1, provides a platform for probing P3HT channel and Au/P3HT contact properties via potential measurements along the P3HT channel during device operation. These measurements using the voltage probes enabled us to measure the sheet conductance of a P3HT film depending on the charge carrier density modulated by the gate voltage applied. From the plot of sheet conductance as a function of gate voltage, the transistor parameters such as the charge carrier mobility and threshold voltage can be measured. This approach separates the metal/semiconductor contact properties from the charge transport properties in the channel.[14] The contact resistance was calculated by subtracting the channel resistance from the total resistance, which can also be derived from the voltage difference between the applied voltages at the source and drain electrodes and the calculated voltages at the Au/P3HT contact determined by extrapolating a linear potential profile along the P3HT channel to the source and drain electrodes.[15]

The two contact FET mobility and threshold voltage were obtained in the linear regime of transistor operation, which is described in eq 1.

$$I_d = \frac{Z}{L}\mu C_{oxide}(V_G - V_T)V_D \quad (1)$$

Here, μ is the two-contact FET mobility, and C_{oxide} is the capacitance per unit area of the silicon oxide gate dielectric. In this paper, we defined μ_{eff} as the effective mobility acquired from the gated sheet conductance measurement to differentiate this value from the conventional two contact FET mobility, μ, from eq 1.

EXPERIMENTAL SECTION

Materials. P3HT was purchased from Sigma Aldrich and used without further purification. The P3HT had a M_n of 24 kD and M_w of 47.7 kD, as obtained from gel permeation chromatography (GPC) of the polymer sample in tetrahydrofuran solution. A Waters 1515 Isocratic high performance liquid chromatography system with a Waters 2489 UV/vis detector, fitted with a Styragel HR 5E column was used. MW data were determined using polystyrene standards. Polymer regioregularity was estimated as 92−94% from the ^{1}H NMR spectrum obtained from deuterated chloroform solution at 293 K using a Bruker DSX.

Fabrication and Characterization of P3HT FETs. Two contact FETs with multiple voltage probes between electrodes were fabricated on SiO_2 substrates on which the source and drain electrodes (Au (50 nm)/Cr (5 nm)) were distanced by 165 μm. The source and drain contacts were fabricated using a standard photolithography based lift-off process, followed by E-beam evaporation (CVC Inc.) of 50 nm Au contacts with 5 nm of Cr as the adhesion layer. For electrical characterization, P3HT films were formed via spin-coating (1500 rpm for 60 s) of a P3HT/chloroform solution prepared with two different concentrations (~3 and ~1 mg/mL) onto 200 nm thick silicon oxide substrates. The P3HT thickness was 15 and 6 nm for the respective solutions and was measured using ellipsometry (M-2000 VASE Ellipsometer, J.A. Woollam Co. Inc.). All the electrical measurements were carried out in ambient air.

Encapsulation of P3HT FETs. To encapsulate the devices, an organic−inorganic hybrid structure of parylene (650 nm) and Al_2O_3 (50 nm) was fabricated with a P3HT semiconducting layer. Parylene was deposited onto the P3HT film to prevent thermal damage during Al_2O_3 film deposition. The Al_2O_3 film was deposited by atomic layer deposition at a temperature of 110 °C in a reactor chamber in which sequential exposures of trimethylaluminum (TMA) and water are performed. TMA and water were pulsed for 15 ms and nitrogen was also used for 5 s to purge the chamber between the TMA and water. This cycle was repeated with a deposition rate of 1 Å/cycle to form a 50 nm thick Al_2O_3 layer.

RESULTS

Degradation of Conjugated Polymers at Gate Dielectric and Metal Contact Interfaces. P3HT/SiO_2 and P3HT/Au interfaces in an FET device fabricated with an ultrathin P3HT layer begin to interact with molecules present in ambient air immediately upon film formation. The change in the electrical properties due to electronic structural changes within the semiconductor is shown in Figure 2. Figure 2a shows time dependence of sheet conductance as a function of gate voltage after P3HT film formation. The slopes and intercepts of the linear fits to the gate voltage axis represent the effective mobility and threshold voltage (Figure 2b) excluding the P3HT/Au contact resistance. This approach to obtain values for the effective

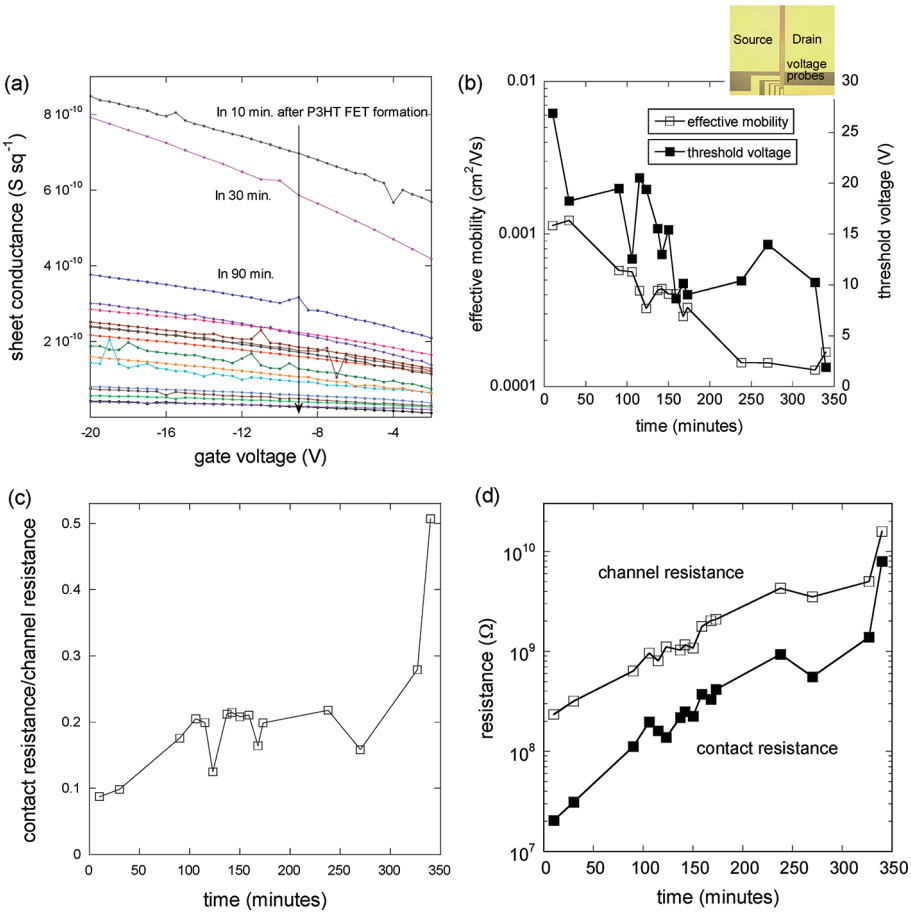

Figure 2. Plots of (a) the sheet conductance vs gate voltage as a function of time in ambient air after formation of a 6 nm thick P3HT film; (b) effective mobility and threshold voltage, (c) contact and channel resistances, and (d) ratio of the contact resistance to the channel resistance vs time in ambient air after fabrication of an FET with a 6 nm thick P3HT film. The inset in b shows an optical micrograph of the FET device with multiple voltage probes between the source and drain electrodes.

mobility and threshold voltage has been previously described.[15] For a device prepared and evaluated in air 20 min after semiconducting film formation, the effective mobility was 1.1×10^{-3} cm^2/(V s), and the mobility was seen to decrease by about 1 order of magnitude after 327 min in the ambient air environment. The threshold voltage varied from 2 to 27 V with a tendency to shift in value toward a more negative direction. The decrease in the threshold voltage was reproducibly observed in the FETs with P3HT films with thickness less than ~10 nm.

Exposure of the ultrathin semiconducting layer to air altered the contact properties as well as the channel properties. The variations in the contact and channel resistances were monitored through analysis of the potential profile along the P3HT channel obtained at the linear regime of transistor operation.[15] In Figure 2c, both the channel and contact resistances are seen to increase with time; the contact resistance increased by more than 2 orders of magnitude from 2.0×10^7 to 8.0×10^9 Ω, while the channel resistance increased by more than 1 order of magnitude from 2.3×10^8 to 1.6×10^{10} Ω. More importantly, as shown in Figure 2d, the ratio of the contact resistance to the channel resistance displayed a dramatic increase of nearly a factor of 3, from 0.16 to 0.51, after 270 min exposure, in contrast to the gradual increase seen at residence times in air of less than 270 min.

The time dependence of the contact resistance is consistent with the estimated voltage drop at the source and drain electrodes via the measured potential profile along the P3HT channel. In Figure 3a, the potential along the P3HT channel is plotted as a function of distance from the source electrode with time in air. The values of the voltage drop at both electrodes, calculated from a linear fit of the potential profile within the P3HT channel, are plotted as a function of time in Figure 3b. The voltage drops at the source and drain electrodes after 10 min of exposure were 0.06 and 0.17 V, respectively. The value of the voltage drop at the source electrode increased almost linearly with time up to a value of 0.87 V, equivalent to a contact resistance of 2.8×10^9 Ω over the same time frame, while the voltage drop at the drain electrode remained almost constant at a value below 0.2 V until 327 min of exposure to air, followed by a rise to 0.4 V. The large asymmetry observed for the voltage drop across the two electrodes was confirmed through repetition of the experiment where the source and drain electrodes were switched. The latter experiment suggests that the large voltage drop observed at the source electrode arises not because of physical defects at the Au/P3HT contact that may arise during device fabrication, but rather, because of an increase in the charge injection barrier at the source electrode.

Encapsulation of the Accumulation Layer with a Layered Hybrid Material. Degradation of performance of FETs fabricated with organic semiconductors has been reported to be mainly due to penetration of water and oxygen molecules into

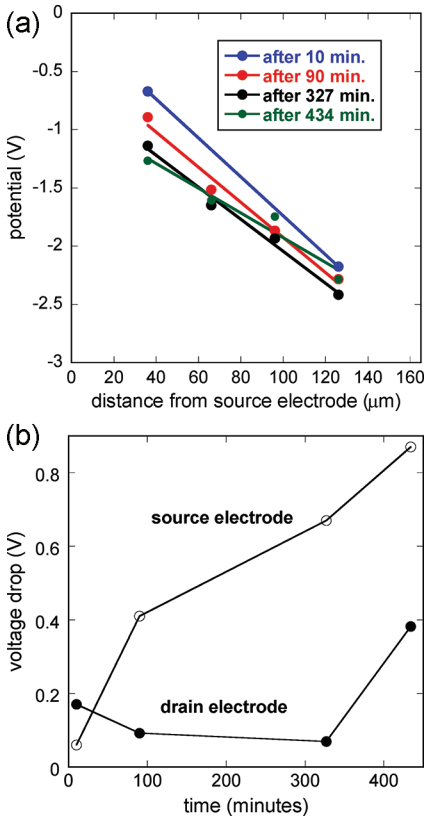

Figure 3. (a) Potential distributions along the P3HT channel as a function of distance from the source electrode with variations in the time of exposure to ambient air. (b) Plots of the voltage drop at the source and drain electrodes as a function of time, in ambient air, after P3HT film formation. The drain voltage was fixed at −3 V.

the active layer of the device.[16−18] Encapsulation of an FET device through introduction of blocking layers onto the active semiconductor should delay the degradation process by retarding permeation of the contaminants into the film. Here, we explored the impact of encapsulation on the performance of P3HT based FET devices. After deposition of the semiconductor, the P3HT films were capped with a 650 nm thick layer of parylene which was used to prevent thermal damage to the P3HT films during subsequent Al_2O_3 deposition at an elevated temperature. A schematic diagram of the encapsulated device configuration is shown in the inset of Figure 4b.

It is evident that the threshold voltage and effective mobility of the encapsulated devices, acquired from the plots of sheet conductance vs gate voltage shown in Figure 4(a), remain constant for a far longer period of time than in the FET without the encapsulation layers, as shown in Figure 4(b). For exposure to the ambient for a period of up to 89 h, both values fluctuated in the narrow ranges of between −6 and 3 V for the threshold voltage and between 0.020 and 0.023 $cm^2/(V\,s)$ for the effective mobility. With increased time, diffusion of water and oxygen from air into the P3HT through the capping layers became apparent. The observed decrease in the effective mobility that occurred between 89 and 906 h of exposure was fit to the equation, $\mu(t) = \mu_0 \exp(-\alpha t)$, affording $\alpha = 6 \times 10^{-4}$, a value which is significantly lower than $\alpha = 0.5$ calculated for the device fabricated with an ultrathin P3HT layer that was not encapsulated (Figure 2b). After 906 h of exposure, the increase in the threshold voltage and decrease in the effective mobility continued, and was coupled with an increase in the contact and channel resistances, as seen in Figure 4c.

The positive shift in threshold voltage in Figure 4b is known to arise from oxygen doping into *p*-channel organic semiconductors, producing acceptor-like states within the band gap of the material.[12] To gain insight into the mechanism of the oxygen induced shift, the dopant density associated with the variation of the threshold voltage in Figure 4b was calculated from the description suggested by Meijer et al.,[16] where the dopant density was estimated from the depletion layer width of an organic semiconducting layer, as given by eq 2.

$$W_{\text{depletion}} = \frac{\varepsilon_0 \varepsilon_{\text{P3HT}}}{C_{\text{oxide}}} \left[\sqrt{1 + \frac{2{C_{\text{oxide}}}^2 (V_G - V_{so})}{q N_A \varepsilon_0 \varepsilon_{\text{P3HT}}}} - 1 \right] \tag{2}$$

Here, ε_0 is the permittivity of vacuum, $\varepsilon_{\text{P3HT}}$ the relative permittivity of P3HT and q the elementary charge. When $V_G - V_{so}$, the difference between the applied gate voltage and the switch-on voltage (V_{so}) defined as the gate voltage at which the drain current begins to increase, reached the pinch off voltage at which no drain current is observed due to complete depletion of the channel, the depletion layer thickness $W_{\text{depletion}}$ is assumed to be equal to the thickness of the P3HT film, allowing for the calculation of the dopant density N_A, as described in eq 3.

$$N_A = \frac{2(V_{so} - V_{fb})\varepsilon_0}{q\left(\frac{d_{\text{P3HT}}^2}{\varepsilon_{\text{P3HT}}} + \frac{2 d_{\text{P3HT}} d_{\text{oxide}}}{\varepsilon_{\text{oxide}}}\right)} \tag{3}$$

Here, V_{fb} is the flat-band voltage, d_{P3HT} and d_{oxide} are thicknesses of the P3HT and oxide, respectively, and $\varepsilon_{\text{oxide}}$ represents the relative permittivity of oxide. The flat-band voltage of −26 V was determined from the switch-on voltage in a P3HT FET maintained in a vacuum environment (~2×10^{-8} Torr) for several days to remove any oxygen contaminants present in the P3HT film. From eq 3, the concentration of acceptor-like states formed in the encapsulated device between 210 and 1680 h of exposure to air is estimated to be $5.4 \times 10^{18}/cm^3$; the number of states is calculated to be $3.3 \times 10^{18}/cm^3$ after 210 h, and it increases to $8.7 \times 10^{18}/cm^3$ at 1680 h in an ambient atmosphere. This estimate is equivalent to the two-dimensional carrier density of $8.1 \times 10^{12}/cm^2$ for a 15 nm thick P3HT film. As a point of comparison, the magnitude of the threshold voltage shift during the period, 21 V, was converted to the two-dimensional charge carrier density described by the equation, $Q = (C_{\text{oxide}}\Delta V_T)/(q)$, giving a value of $2.3 \times 10^{12}/cm^2$. Evaluation of the dopant density and the threshold voltage shift suggests that approximately 30% of the number of states created within the band gap of P3HT participated in shifting the threshold voltage, assuming that the threshold voltage shift is related to charged states at the gate dielectric/organic semiconductor interface.[17] Figure 4c additionally shows that encapsulation of the device prevented airborne water and oxygen from permeating to the P3HT/Au interface as well as the P3HT channel. Note that the trend of the changes in the contact resistance is similar to those of the channel resistance.

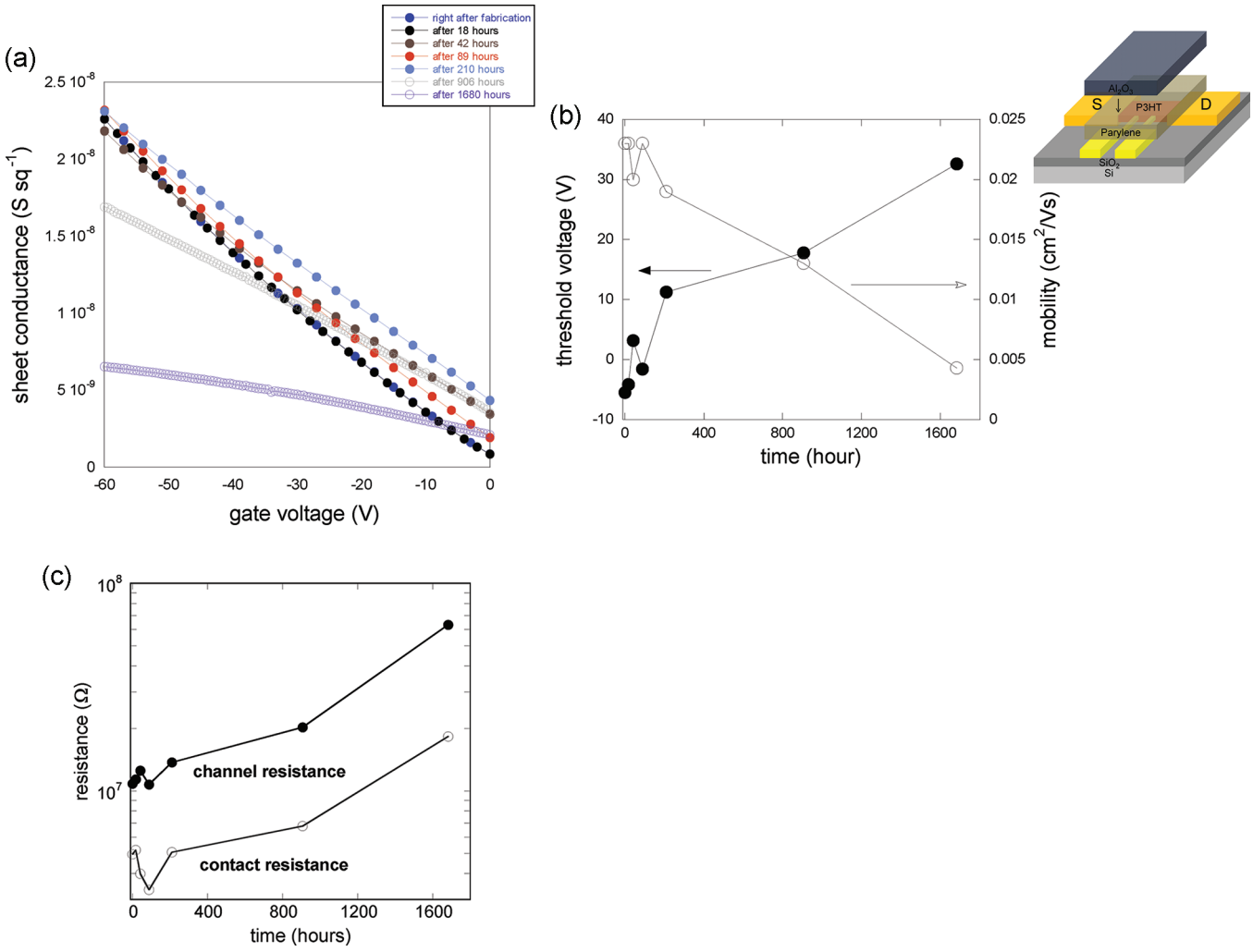

Figure 4. (a) Plots of sheet conductance as a function of gate voltage for an encapsulated P3HT based FET with extended exposure to ambient air. Plots of (b) threshold voltage and effective mobility and (c) contact and channel resistances as a function of time in ambient air after fabrication of a P3HT FET with encapsulation layers. The inset in b shows a schematic diagram of the FET device with the encapsulation layers. The thickness of the P3HT film was 15 nm, and the drain voltage was −3 V.

DISCUSSION

The change in the mobility and threshold voltage in air, independent of the P3HT/Au contact properties, determines the decay rate of the P3HT channel sheet conductance. For an FET prepared with a thin P3HT semiconducting film (Figure 2), whose thickness is comparable to the accumulation layer thickness of several nanometers, the characteristic time of the decay, τ = 69 min, acquired from the stretched-exponential function of $\sigma_{\square}(t) = \sigma_{\square}(0)\exp(-(t/\tau)^{\gamma})$ is much smaller than τ = 625 min obtained for a 25 nm thick film (data not shown). This result clearly shows that interaction of charge carriers within the two-dimensional charge transport sheet with selected molecular species in air was more efficient in the thin film device than for a device prepared with a thick semiconducting layer where airborne molecules must first diffuse through upper layers of the material in order to reach the accumulation layer. With encapsulation, the sheet conductance fluctuated between 3 and 7×10^{-9} S sq^{-1} due to an increase in carrier density, i.e., threshold voltage increase, occurring with a decrease in the mobility. This behavior is distinctive and is discussed below. It is noted that in explaining the origin of the sheet conductance decay, bias stress instability caused by the presence of charge trapping sites within the polymer film can be ruled out because the time interval between measurements ensured sufficient time for trapped carriers to recover to their original states.[18,19]

The change in charge transport properties in air influenced the contact properties, particularly the charge injection barrier at the source electrode, as seen in panels a and b in Figure 5. The plots acquired from the time dependent mobility and contact resistance measurements for the devices fabricated with a thin P3HT film without encapsulation (Figures 2, 3, and 5a) and a thick P3HT film with encapsulation (Figures 4 and 5b) show that the contact resistance increased with decreasing mobility. It has been demonstrated that the net injection current in disordered organic materials, which is the difference between the injected current across the metal/P3HT contact and the surface recombination current from organic material to metal,[20,21] is governed by the charge carrier mobility as expressed by $J_{inj} = 4\psi^2 N_0 e\mu E \exp(-\varphi_B/kT)\exp(f^{1/2})$. In that relation, the net injection current is proportional to the electric field, E, and the charge carrier mobility, μ. The linear fits depicted in panels a and b in Figure 5 suggest a power law dependence of the contact resistance on

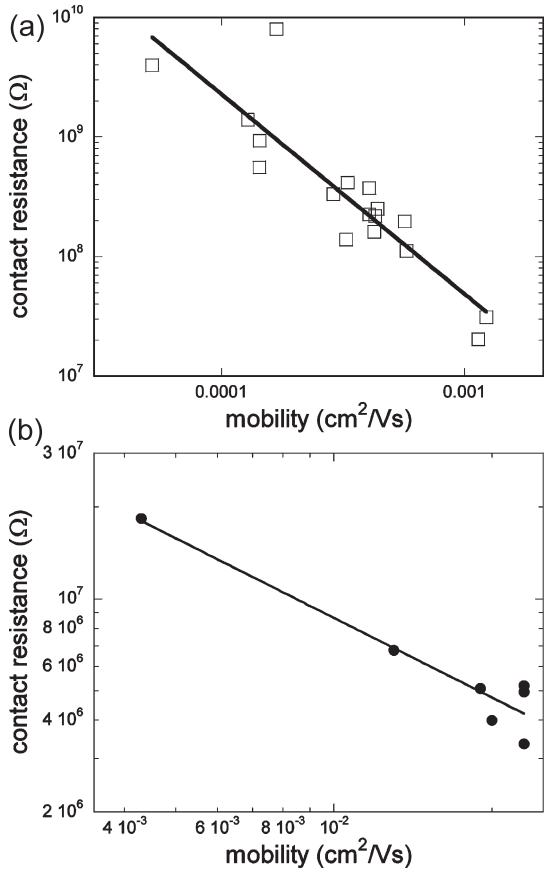

Figure 5. Plots of contact resistance vs mobility for FETs fabricated with (a) a 6 nm thick P3HT film without encapsulation, and (b) a 25 nm thick P3HT film encapsulated with a hybrid organic/inorganic structure.

mobility with exponents of 1.7 and 0.9, respectively. These values are in good agreement with a power law dependence of the contact resistance and mobility, $R_{con} \approx \mu^{-1}$, derived from the above equation. The contact resistance is thus dominated by charge injection which is limited by diffusion of charge carriers at the metal/P3HT contact. In addressing the origin of the change in the contact resistance with time, we can rule out the contribution of the bulk transport of injected carriers in P3HT through the route to the accumulation layer near SiO_2 because a thin P3HT film (~6 nm) was used as the active layer.[22] Surface oxidation of the Cr adhesion layer, however, can influence the contact resistance despite the correlation between the injection barrier and the mobility.[22] The low voltage drop, observed in Figure 3b, at the source electrode immediately after P3HT film formation is consistent with a low hole injection barrier of ~0.1 eV.[23]

Increase in the ratio of the contact resistance to the channel resistance is found to occur with time Figure 2d. The appearance of the contact limited regime began with the large voltage drop at the drain electrode, as clearly seen in Figures 2d and 3b. Unlike the instant increase in the voltage drop at the source electrode, the delayed occurrence of the large voltage drop at the drain electrode is associated with the thickness of the P3HT layer. In our experiments, a large voltage drop at the drain electrode was observed for devices prepared with ~2 nm thick P3HT films immediately after film formation. For those devices having semiconductor films thicker than 50 nm, a contact limited regime was not observed within the lifetime of the devices. This thickness dependence of the onset of a voltage drop at the drain electrode suggests that the large contact resistance at the drain electrode arises from the interaction between airborne species and the P3HT semiconductor near the Au/P3HT contact region close to the SiO_2 gate dielectric. As the thickness decreases, more localized electronic states near the source and drain contacts can be readily created in the P3HT via more direct contact with molecules such as oxygen present in the air ambient. Hole transport within the p-channel in the linear regime of transistor operation is more severely limited by the presence of trapping sites near the drain electrode due to fewer carriers than are present near the source electrode. The deficiency of hole carriers at the drain electrode limits either diffusion or drift of charge carriers into the drain electrode. Indeed, a large contact resistance at the drain electrode has been reported in FETs having highly disordered semiconducting films.[22,24] The observations noted above lead to the conclusion that a certain critical number of molecules in air have to diffuse into the charge transport layer near the drain electrode interfacing with the gate dielectric to attain the contact limited regime.

Interestingly, the encapsulation layer enabled selective doping into the P3HT layer, serving as a blocking layer for a particular dopant in air. With encapsulation, the threshold voltage shifted in a positive direction, while the direction of the shift was negative when no encapsulation was used. This trend was reproducibly observed for multiple samples. It is believed that the direction of the change in the threshold voltage is associated with the particular dopants. Information pertaining to the effects of water and oxygen on the device parameters, such as the threshold voltage and mobility, is available.[12,17] Water has been reported to be the main source for the shift of the threshold voltage to a more negative value in FETs using p-channel organic semiconductors, while the opposite has been reported for oxygen.[11,12,25] However, to identify a particular dopant that shifts the threshold voltage in a particular direction, more experiments in controlled environments are required.

SUMMARY AND CONCLUSION

We clearly demonstrated that charge carriers in the accumulation layer of transistor structures interact with molecules in air which results in a change in the P3HT channel and P3HT/Au contact properties. The decrease in the effective mobility of a P3HT semiconductor film led to an increase in the contact resistance, with the recombination current from P3HT to the metal electrode increasing. The increase in the charge injection barrier at the source electrode contributed to the observed increase in the contact resistance in air, and was accompanied by an abrupt rise in the charge extraction barrier at the drain electrode rendering the FETs contact limited. When the devices were encapsulated, the main substance affecting the P3HT active layer was different from that impacting the unencapsulated device.

FET device architectures can provide an elementary test structure to aid in understanding the performance degradation mechanisms of semiconducting polymers in air via the change in device parameters. The results presented here have applications in the design and engineering of the metal/semiconductor contact and semiconductor/gate dielectric interface, as well as the design of encapsulation structures; optimization of these components will impact the development of air stable devices fabricated with organic or polymeric semiconductors.

AUTHOR INFORMATION

Corresponding Author
*E-mail: ereichmanis@chbe.gatech.edu (E.R.); bp288@cornell.edu (B.P.).

ACKNOWLEDGMENT

This research was funded in part by the Center for Organic Photonics and Electronics (COPE), Georgia Tech, by the CMDITR STC Program of the National Science Foundation (DMR-0120967), and the Center for Interface Science: Solar Electric Materials (CIS:SEM), an Energy Frontier Research Center funded by the U.S. Department of Energy, Office of Science, Office of Basic Energy Sciences under Award Number DE-SC0001084 (Yongjin Kim for work on barrier films).

REFERENCES

(1) Torsi, L.; Dodabalapur, A.; Rothberg, L. J.; Fung, A. W. P.; Katz, H. E. *Science* **1996**, *272*, 1462–1464.
(2) Peumans, P.; Yakimov, A.; Forrest, S. R. *J. Appl. Phys.* **2003**, *93*, 3693–3723.
(3) Gross, M.; Muller, D. C.; Nothofer, H. G.; Scherf, U.; Neher, D.; Brauchle, C.; Meerholz, K. *Nature* **2000**, *405*, 661–665.
(4) Gunes, S.; Neugebauer, H.; Sariciftci, N. S. *Chem. Rev.* **2007**, *107*, 1324–1338.
(5) Meijer, E. J.; de Leeuw, D. M.; Setayesh, S.; van Veenendaal, E.; Huisman, B. H.; Blom, P. W. M.; Hummelen, J. C.; Scherf, U.; Kadam, J.; Klapwijk, T. M. *Nat. Mater.* **2003**, *2*, 678–682.
(6) Ong, B. S.; Wu, Y. L.; Liu, P.; Gardner, S. *J. Am. Chem. Soc.* **2004**, *126*, 3378–3379.
(7) Dennler, G.; Lungenschmied, C.; Neugebauer, H.; Sariciftci, N. S.; Labouret, A. *J. Mater. Res.* **2005**, *20*, 3224–3233.
(8) Jorgensen, M.; Norrman, K.; Krebs, F. C. *Sol. Energy Mater. Sol. Cells* **2008**, *92*, 686–714.
(9) Pannemann, C.; Diekmann, T.; Hilleringmann, U. *J. Mater. Res.* **2004**, *19*, 1999–2002.
(10) Kagan, C. R.; Afzali, A.; Graham, T. O. *Appl. Phys. Lett.* **2005**, *86*, 193505.
(11) Chabinyc, M. L.; Endicott, F.; Vogt, B. D.; DeLongchamp, D. M.; Lin, E. K.; Wu, Y. L.; Liu, P.; Ong, B. S. *Appl. Phys. Lett.* **2006**, *88*, 113514.
(12) Abdou, M. S. A.; Orfino, F. P.; Son, Y.; Holdcroft, S. *J. Am. Chem. Soc.* **1997**, *119*, 4518–4524.
(13) Jurchescu, O. D.; Baas, J.; Palstra, T. T. M. *Appl. Phys. Lett.* **2005**, *87*, 052102.
(14) Devine, R. A. B. *J. Appl. Phys.* **2006**, *100*, 034508.
(15) Park, B.; Aiyar, A.; Hong, J. I.; Reichmanis, E. *ACS Appl. Mater. Interfaces* **2011**, *3*, 1574–1580.
(16) Meijer, E. J.; Detcheverry, C.; Baesjou, P. J.; van Veenendaal, E.; de Leeuw, D. M.; Klapwijk, T. M. *J. Appl. Phys.* **2003**, *93*, 4831–4835.
(17) Gu, G.; Kane, M. G.; Mau, S. C. *J. Appl. Phys.* **2007**, *101*, 014504.
(18) Sirringhaus, H. *Adv. Mater.* **2009**, *21*, 3859–3873.
(19) Mathijssen, S. G. J.; Colle, M.; Gomes, H.; Smits, E. C. P.; de Boer, B.; McCulloch, I.; Bobbert, P. A.; de Leeuw, D. M. *Adv. Mater.* **2007**, *19*, 2785–2789.
(20) Emtage, P. R.; Odwyer, J. J. *Phys. Rev. Lett.* **1966**, *16*, 356–358.
(21) Scott, J. C.; Malliaras, G. G. *Chem. Phys. Lett.* **1999**, *299*, 115–119.
(22) Burgi, L.; Richards, T. J.; Friend, R. H.; Sirringhaus, H. *J. Appl. Phys.* **2003**, *94*, 6129–6137.
(23) Thakur, A. K.; Mukherjee, A. K.; Preethichandra, D. M. G.; Takashima, W.; Kaneto, K. *J. Appl. Phys.* **2007**, *101*, 104508.
(24) Li, T.; Ruden, P. P.; Campbell, I. H.; Smith, D. L. *J. Appl. Phys.* **2003**, *93*, 4017–4022.
(25) Hoshino, S.; Yoshida, M.; Uemura, S.; Kodzasa, T.; Takada, N.; Kamata, T.; Yase, K. *J. Appl. Phys.* **2004**, *95*, 5088–5093.